

# Fluidized Bed Gasification of Biomass Char by Chemical Looping

Francesco Miccio<sup>a,\*</sup>, Elettra Papa<sup>a</sup>, Annalisa Natali Murri<sup>a</sup>, Elena Landi<sup>a</sup>, Valentina Medri<sup>a</sup>, Angelo Vaccari<sup>a,b</sup>

<sup>a</sup>Istituto di Scienza e Tecnologia dei Materiali Ceramici (ISTEC) - CNR, via Granarolo, 64, 48018 Faenza, Italy

<sup>b</sup>Dipartimento di Chimica Industriale "Toso Montanari", Alma Mater Studiorum – Università di Bologna, via Risorgimento 4, Bologna

[francesco.miccio@cnr.it](mailto:francesco.miccio@cnr.it)

Biomass gasification is a green and effective process to generate synthesis gas (syngas, CO + H<sub>2</sub>) with high heating value provided that inert species (e.g. N<sub>2</sub>) are removed from the products or inherently avoided in the feedstock. In this respect, the combination of oxygen gasification and pre-pyrolyzed biomass is extremely favourable for issuing a gas stream with high CO and H<sub>2</sub> content that can be further converted to valuable chemicals. The application of chemical looping schemes permits O<sub>2</sub> transfer from air to the reaction chamber via oxygen carriers, namely metal oxides having multiple oxidation states, without contemporary transfer of N<sub>2</sub>. In this manuscript the results of preliminary tests of chemical looping gasification are reported and discussed. The experiments were made at 900 °C with a synthetic oxygen carrier based on copper oxide. The conversion of biomass char to CO was investigated in batch-type tests providing insights into optimization of gasification atmosphere and oxygen carrier regeneration.

## 1. Introduction

Biomass gasification is a green and reliable process for generation of a synthetic gas with high heating value provided that inert species, in particular nitrogen present in the air, are removed from the products or inherently avoided in the feedstock (Ruoppolo et al., 2013). In this respect, the combination of oxygen gasification and pre-pyrolyzed biomass is extremely favourable for issuing a gas stream with high content in CO and H<sub>2</sub> that can be further converted into valuable chemicals or energy by internal combustion engines or fuel cells (Bridgewater, 1995). However, the utilization of an air separation unit is not advised from economic point of view in typical small-medium scale biomass fuelled plants, in scale of 1-10 MW<sub>e</sub>. The allothermal process based on steam gasification is a possible option, requiring heat supply from an external source and a circulating fluidized bed (FB) configuration (Basu, 2006). In alternative, the application of the emerging chemical looping technology permits oxygen transfer from air to the gasification chamber via an oxygen carrier (OC), without contemporary transfer of N<sub>2</sub>, with inherent enrichment of the produced gas (Lyngfelt, 2013).

Apart from natural metal oxides (e.g. hematite, ilmenite), synthetic or modified oxygen carriers based on Ni, Fe, Mn and Cu have been investigated, for instance sintered NiO-Al<sub>2</sub>O<sub>3</sub> (Bolh ar-Nordenkampf et al., 2009), Fe<sub>2</sub>O<sub>3</sub> on alumina support (Cabello et al., 2014); CuO promoted by Mn<sub>2</sub>O<sub>3</sub> (Hosseini et al., 2015); Mn-Fe mixed oxides prepared by hydrothermal synthesis (Lambert et al., 2009); promoted Fe and Mn ores by dry impregnation (Haider et al., 2016); and, recently, Mn-Fe oxides (Miccio et al., 2018) and CuO powder (Natali Murri et al., 2020) inside a geopolymer (GP) matrix. In this respect, the geopolymer synthesis is based on a one-step protocol operating at low temperature (below 100 °C) by chemical consolidation of an alkali-aluminosilicate slurry forming the GP matrix (Medri et al., 2013).

In chemical looping gasification (CLG) the lattice oxygen in the carrier convert the fuel. The carrier continuously supplies oxygen for gasification with redox cycle and behaves as a good catalyst for tar cracking. However, there are still few investigation reported in literature about biomass CLG (Lin et al., 2020).

This paper reports the experimental results of CLG in a bench-scale FB reactor. The bed was given by composite particles of GP and CuO, purposely prepared. As preliminary investigation, the biomass was pre-

devolatilized in order to remove any effect deriving from the fast release of volatiles from fed particles. The outcomes of CLG experiments, as well as the microstructural characterization of the samples obtained from the tests are presented and discussed.

## 2. Methods

### 2.1 Materials

A synthetic oxygen carrier (OC), classified as GPCuO, was prepared by mixing CuO powder, having specific BET surface area values of  $8.8 \text{ m}^2/\text{g}$ , with a GP according to a previously-developed formulation (Natali Murri et al., 2020) by mechanical stirring for 10 min. The geopolymer composite was then cast in sealed silicone molds and cured at  $80 \text{ }^\circ\text{C}$  for 24 h, followed by 24 h curing at room temperature. Finally, the metal oxide-GP monoliths were roughly crashed in a porcelain mortar, and the obtained granules were sieved in the desired grain size fraction of 0.2-0.4 mm for utilization in fluidized bed. The granulate was then conditioned by calcining at  $900 \text{ }^\circ\text{C}$  in air for 2h. The final content of active metal oxide in the material, calculated by XRF analysis on calcined granulates was slightly lower than 40% wt.

Alternative materials for FB tests were quartzite and chromite sand in similar sizes. In some tests fireclay was added to limit agglomeration phenomena.

### 2.2 Instrumental characterization

The morphology and macrostructure of GPCuO granules were investigated by digital microscopy (3D Digital Microscope RH2000, Hirox, Japan). Microstructural features were examined by a field emission gun-scanning electron microscope (FE-SEM, SIGMA: Zeiss, Germany) equipped with energy dispersion spectroscopy (EDS-Oxford Instruments). X-ray diffraction analysis was carried out by Bruker D8 Advance powder diffractometer (Karlsruhe, Germany) with CuK $\alpha$  radiation.

### 2.3 Experimental apparatus and techniques

A bench-scale bubbling fluidized bed reactor was used for CLG tests under atmosphere of  $\text{CO}_2$  and  $\text{CO}_2/\text{N}_2$ . The fluidization column was formed by an alumina tube with internal diameter of 28 mm and 500 mm high. The gas distributor was formed by a layer of compacted ceramic fibers at the bottom of the tube. The top end of the column was accessible for temperature measurement by a K type thermocouple, fuel feeding and gas sampling, as shown in Figure 1. The reactor was installed in a Watlow (USA) ceramic furnace provided with electronic control of temperature.

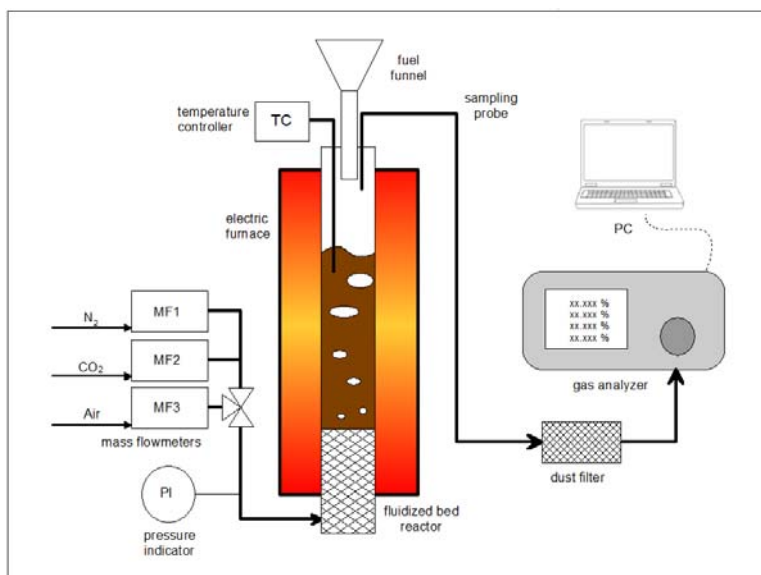


Figure 1: Experimental setup for fluidized bed gasification.

The flow rates of air,  $\text{N}_2$  and  $\text{CO}_2$  were supplied by means of manual and electronic flowmeters (Brooks, mod. 5850S); fittings and valves allowed for the fast switch of the gas stream. A TESTO analyzer (mod. 350,

Germany) was used for continuous measurements of  $O_2$ ,  $CO_2$  and  $CO$  at the exit of the gasifier. The gas was sampled by means of a 6 mm AISI 316 probe, at middle position of the fluidization column.

The fuel was quickly fed in batches (0.2 or 0.5 g) from the top side throughout a glass funnel. The fuel was char of beech wood produced under  $N_2$  atmosphere at  $800\text{ }^\circ\text{C}$  and sieved in the particle size 1.0-2.0 mm. The residual ash content was 3%wt. as determined by thermogravimetry.

### 3. Results

#### 3.1 Sample characterization

SEM images of GPCuO-fireclay granules are shown in Figure 2. The GP grains appear homogeneous in their macrostructure, and don't exhibit any significant effect from the cycling conditions. They still maintain sharp edges (Figure 2-A) and no visible cracks may be detected, suggesting that crystallization of the GP paste into leucite phase did not give rise to any detrimental volume alteration, preserving the material.

The microstructure of the grain surface after cycling (Figure 2-B) shows a well reacted and uniform matrix, where CuO particles can be detected, well dispersed in the matrix. Local effects of grain coalescences and necks formation may be evidenced (Figure 2-C), owing to the presence of melted glassy phases deriving from the amorphous silicate phases of the geopolymer.

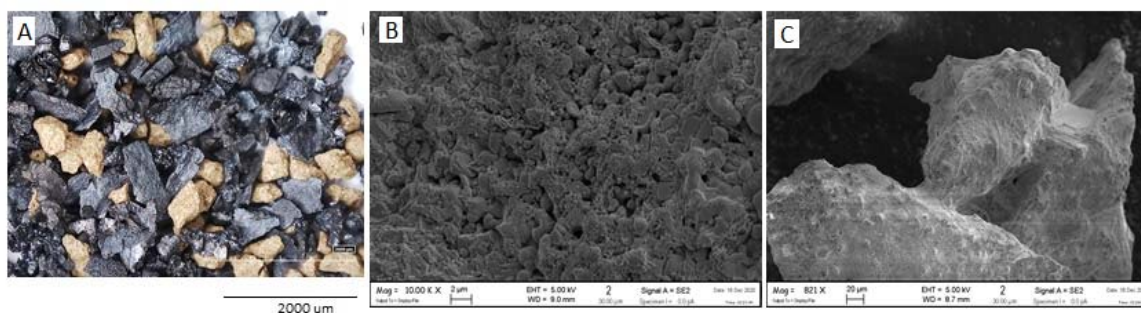


Figure 2: High resolution images of GPCuO granules after cycling: A) dark granules are GPCuO while light granules are fireclay; B) microstructure; C) coalescence between two granules .

XRD analysis (Figure 3) of GPCuO granules after cycling and cooling in air clearly evidences the starting CuO phase, leucite belonged to the thermal transformation of GP phase while quartz was an impurity of the metakaolin used to produce the geopolymer.

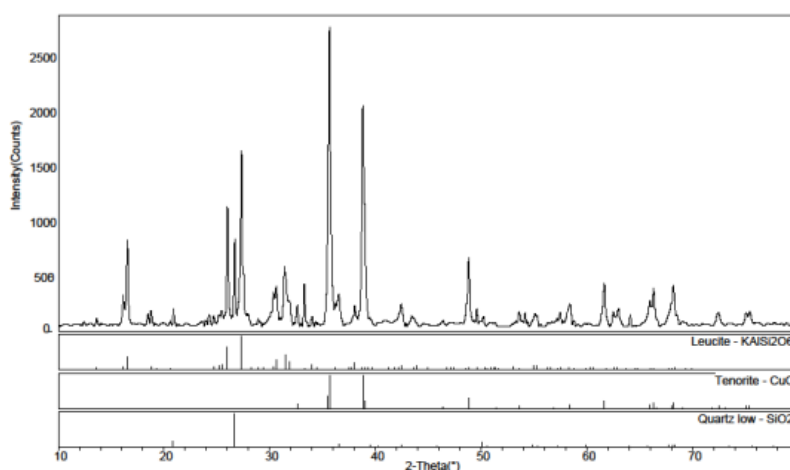
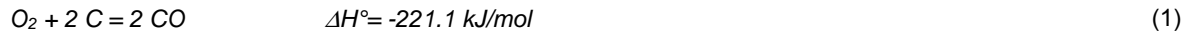


Figure 3: XRD analysis of GPCuO granules after cycling.

### 3.2 Results of CLG gasification

Figure 4 shows the CO profile along the time-on-stream obtained during a test feeding multiple batches of char, alternated to regeneration steps in air. All gasification trials were done in CO<sub>2</sub>/N<sub>2</sub> (50/50 v/v %) atmosphere. Upon the switch from air to CO<sub>2</sub>/N<sub>2</sub> and contemporary char feeding ( $W_{ch}=0.50$  g), a peak in CO concentration appears, followed by a slow decay of its profile. Notably, first (time 600 s) and second (time 4400 s) peaks are very similar, indicating an effective regeneration of the oxygen carrier (GPCuO) during the step in air. Conversely, the third char supply at 5,700 s gave rise to a larger CO peak, again declining slowly, as the previous ones. It is worth noting that the switch to air at 2,500 and 8,100 s suddenly dropped the CO concentration to zero, because of the very fast combustion of char at 900 °C.



The difference noted in CO peaks after OC regeneration and without regeneration is attributable to the exhaustion of the carrier, becoming less able to supply oxygen for the char partial oxidation, Eq(1). Thus, the char conversion occurred also via C gasification by CO<sub>2</sub>, reverse Boudouard reaction Eq(2), giving high yield in CO. Of course, this mechanism is more efficient in order to produce a more energetic gas, because of the higher CO content, but it requires external heat, reaction Eq(2) being endothermic.

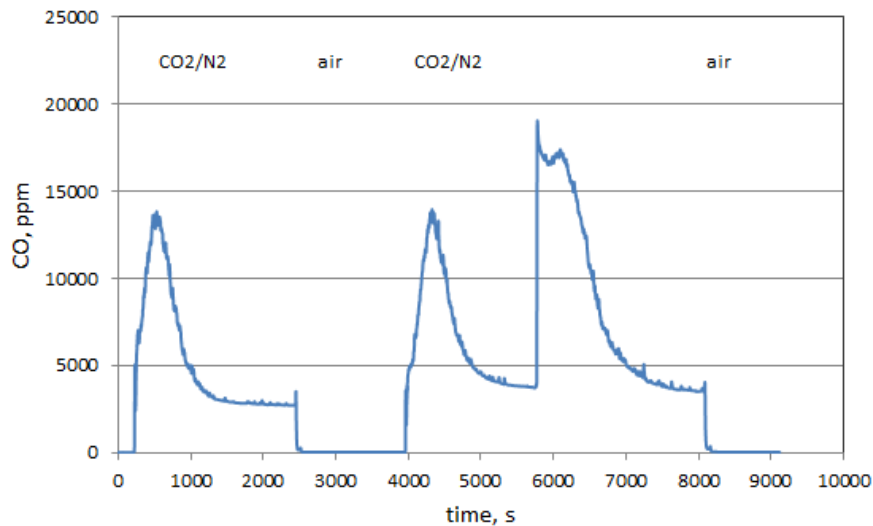


Figure 4: CO concentration for sequential feeds of beech char in CO<sub>2</sub>/N<sub>2</sub> (50/50 %vol),  $W_{ch}=0.50$  g,  $T=900$  °C (GPCuO).

The integration of CO profiles over the time, Eq(4), allowed the computation of CO yield for each char batch, where P and Q are pressure and volumetric flowrate, respectively.

$$n_{CO} = \int_{t_1}^{t_2} PQ \frac{CO_{ppm}/10^6}{RT} dt \quad (4)$$

The results of a preliminary series of tests carried out under different operating conditions and  $T=900$  °C are reported in Table 1. Three different bed materials, quartzite, GPCuO and chromite, were compared in terms of CO yield and CO/C ratio, the latter being also shown in Figure 5. Quartzite is chemically stable and inert, so the obtained results of CO yield and CO/C ratio (row 1) are basically attributable to the heterogeneous reaction Eq(2), representing the baseline for the other tests. The tests with GPCuO under same conditions (rows 2 and 3) gave rise to a marked increase of CO yield because of the concurrent reaction Eq(2). However, the full conversion of C to CO<sub>2</sub> may also occur, Eq(3), due to the oxygen availability from the regenerated oxygen carrier, lowering the conversion of C to CO.

The GPCuO test #4 was conducted without OC regeneration (see Figure 4) and resulted in the highest CO/C ratio (Figure 5). This is likely due to the lower equivalence ratio achieved in this test, since the oxygen carrier was partly reduced at beginning of the test.

Table 1: Summary of gasification tests in fluidized bed ( $T=900\text{ }^{\circ}\text{C}$ )

Test #	Bed material	Gasification stream	Char weight, g	CO yield, mol	CO/C, -
1	Quartzite	CO <sub>2</sub> /N <sub>2</sub>	0.20	0.0043	0.27
2	GPCuO	CO <sub>2</sub> /N <sub>2</sub>	0.50	0.040	0.99
3	GPCuO	CO <sub>2</sub> /N <sub>2</sub>	0.50	0.050	1.24
4	GPCuO	CO <sub>2</sub> /N <sub>2</sub>	0.50*	0.070	1.73
5	GPCuO	CO <sub>2</sub>	0.50	0.061	1.51
6	GPCuO	N <sub>2</sub>	0.20	0.0011	0.027
7	Chromite	CO <sub>2</sub> /N <sub>2</sub>	0.53	0.043	0.81

\* test without OC regeneration

Test #6 of Table 1, corresponding to bar d in Figure 5, was carried out with GPCuO under inert conditions (N<sub>2</sub>) yielding the lowest value of CO/C ratio. In fact, under this conditions the OC promptly released O<sub>2</sub> (Natali Murri et al., 2020) giving rise to full conversion of the char to CO<sub>2</sub>, in absence of the thermodynamic limitation exerted by the presence of CO<sub>2</sub> in the feeding. As alternative, chromite, natural ore containing around 75% of Cr and Fe oxides, was tested (#7) exhibiting a lower performance with respect to GPCuO, in spite of a higher content in reducible oxides. However, chromite was proven to be more resistant to the occurrence of agglomeration phenomena among bed particles, that were experienced with GPCuO (Figure 2c).

Altogether, the trade-off between partial and full oxidation, i.e. reactions Eq(1) and Eq(3), and the concurrent CO<sub>2</sub> gasification reaction Eq(2) played a relevant role in achieving high CO/C ratio. From the point of view of chemical conversion to CO, the reaction Eq(2) offers the highest figure but is kinetically limited and strongly endothermic. A good compromise is given by adopting a mixed atmosphere of CO<sub>2</sub> and O<sub>2</sub>, the latter being provided by the oxygen carrier, where the exothermic reactions Eq(1) and Eq(3) provide heat for endothermic reaction Eq(2). Under this conditions, CO/C ratio between 1.0 and 1.5 may be likely achieved as shown by the reported tests (Table1 and Figure 5).

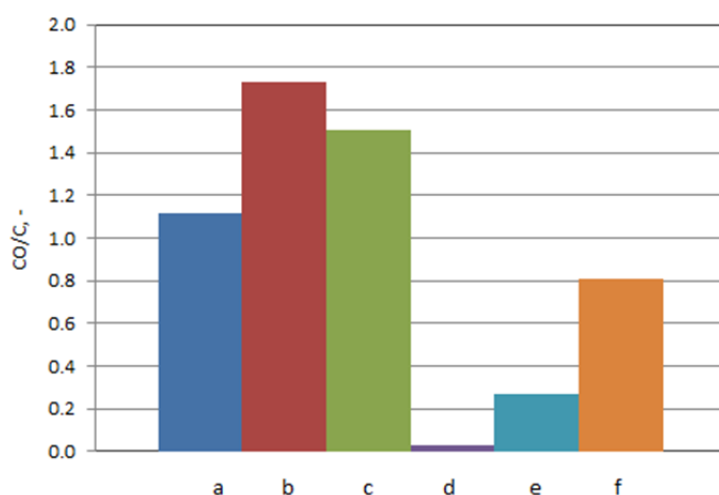


Figure 5: CO/C ratio (mol/mol) for different test conditions. a) GPCuO single batch CO<sub>2</sub>/N<sub>2</sub>; b) GPCuO sequential batch CO<sub>2</sub>/N<sub>2</sub>; c) GPCuO single batch CO<sub>2</sub>; d) GPCuO single batch N<sub>2</sub>; e) quartzite single batch CO<sub>2</sub>/N<sub>2</sub>; f) chromite single batch CO<sub>2</sub>/N<sub>2</sub>.

#### 4. Conclusions

A geopolymer oxygen carrier was prepared by inclusion of copper oxide particles (up to 33 wt. %) inside the matrix following a protocol developed in previous work. The oxygen carrier was tested in fluidized bed at 900 °C in alternating oxidizing and reducing atmosphere, as well as in presence of biomass char.

The main focus was on CO yield and CO/C ratio, as resulted from the analysis and elaboration of the gas issuing from the gasifier. A good result was obtained by adopting a mixed atmosphere of N<sub>2</sub>, CO<sub>2</sub> and O<sub>2</sub>, the latter being provided by the oxygen carrier, where the exothermic reactions of char oxidation provide heat for endothermic C gasification by CO<sub>2</sub>. Under this conditions, CO/C ratios between 1.0 and 1.7 were achieved.

The microstructure of the grain surface after tests shows a well reacted and uniform matrix, where CuO particles can be detected in the matrix, along with presence of melted glassy phases deriving from the amorphous silicates of the geopolymer. Further, no cracks were present demonstrating adequate mechanical resistance and refractoriness of the granules.

#### Acknowledgments

This research has been carried out based on economies of closed projects.

#### References

- Basu P. (Ed.), 2006, *Combustion and Gasification in Fluidized Beds*, Taylor & Francis Group, LLC
- Bolhàr-Nordenkamp J., Pröll T., Kolbitsch P., Hofbauer H., 2009, Performance of a NiO-based oxygen carrier for chemical looping combustion and reforming in a 120 kW unit, *Energy Procedia*, 1, 19-25.
- Bridgewater A.V., 1995, The Technical and Economical Feasibility of Biomass Gasification for Power Generation, *Fuel*, 74, 631-653
- Cabello A., Gayan P., Garcia-Labiano F., de Diego L.F., Abad A., Adanez J., 2016, On the attrition evaluation of oxygen carriers in Chemical Looping Combustion, *Fuel Process. Technol.*, 148, 188-197.
- Haider S.K., Azimi G., Duan L., Anthony E.J., Patchigolla K., Oakey J.E., Leion H., Mattisson T., Lyngfelt A., 2016, Enhancing properties of iron and manganese ores as oxygen carriers for chemical looping processes by dry impregnation, *Appl. Energy*, 163, 41-50.
- Hosseini D., Imtiaz Q., Abdala P.M., Yoon S., Kierzkowska A.M., Weidenkaff A., Müller C.R., 2015, CuO promoted Mn<sub>2</sub>O<sub>3</sub>-based materials for solid fuel combustion with inherent CO<sub>2</sub> capture, *J. Mater. Chem. A*, 3, 10545-10550.
- Lambert A., Delqu   C., Cl  mene  on I., Comte E., Lefebvre V., Rousseau J., Durand B., 2009, Synthesis and characterization of bimetallic Fe/Mn oxides for chemical looping combustion, *Energy Procedia*, 1, 375-381
- Lin Y., Wang H., Wang Y., Huo R., Huang Z., Liu M., Wei G., Zhao Z., Li H., Fang Y., 2020, Review of Biomass Chemical Looping Gasification in China, *Energy Fuels*, 34, 7847-7862.
- Lyngfelt A., 2013, Chemical looping combustion (CLC), in *Fluidized Bed Technologies for Near-Zero Emission Combustion and Gasification* (Ed. F. Scala), Woodhead Pebl., 895-930
- Miccio F., Landi E., Medri V., Papa E., Natali Murri A., 2020, Chemical Looping Gasification of Biomass in a Bed of Geopolymeric Oxygen Carrier, *Chem. Eng. Trans.* 80, 253-258.
- Natali Murri A., Miccio F., Medri V., Landi E., 2020, Geopolymer-composites with thermomechanical stability as oxygen carriers for fluidized bed chemical looping combustion with oxygen uncoupling, *Chem. Eng. J.*, 393, 124756
- Ruoppolo G., Miccio F., Brachi P., Picarelli A., Chirone R., 2013, Fluidized Bed Gasification of Biomass and Biomass/Coal Pellets in Oxygen and Steam Atmosphere, *Chem. Eng. Trans.* 32, 595-600.